Direct coupling of Nod factor signaling to legume vesicular trafficking: A key event in nodulation initiation

Gary Stacey

staceyg@missouri.edu

University of Missouri https://orcid.org/0000-0001-5914-2247

Jae hyo Song

University of Missouri

Mengran Yang

University of Missouri https://orcid.org/0000-0001-5820-9868

Gabriel Jorge

University of Missouri

Daewon Kim

University of Missouri

Shin-Ichiro Agake

University of Missouri

Jeremiah Traeger

Pacific Northwest National Laboratory

Dehong Hu

Pacific Northwest National Laboratory https://orcid.org/0000-0002-3974-2963

Jay Thelen

University of Missouri https://orcid.org/0000-0001-5995-1562

Biological Sciences - Article

Keywords: kinase client assay, Phosphorylation, Clathrin-mediated endocytosis, Infection thread initiation, Legume–rhizobium symbiosis, Soybean nodulation, SNARE complex regulation

Posted Date: December 4th, 2025

DOI: https://doi.org/10.21203/rs.3.rs-8135811/v1

Additional Declarations: There is **NO** Competing Interest.

Abstract

Legume–rhizobium symbiosis relies on the precise integration of receptor-mediated signaling with dynamic membrane trafficking to initiate infection threads (ITs) and accommodate bacterial infection via root hairs. Here, we identify the soybean Qa-SNARE GmSYNTAXIN111a (GmSYP111a), a close paralog of the cytokinesis-specific protein KNOLLE, as a critical regulator in symbiotic infection. A kinase client (KiC) assay revealed that GmSYP111a is a direct phosphorylation substrate of the receptor kinase GmSymRKβ (also known as *DMI2* or *NORK* in other legumes), which modifies Ser-8 at its N-terminus. BiFC, co-immunoprecipitation, and *in vitro* kinase assays confirmed that GmSymRKβ phosphorylates GmSYP111a without disrupting their basal association, but phosphorylation alters the subcellular distribution of the complex. In soybean root hairs, GmSYP111a and GmSymRKβ co-localize to the plasma membrane, and Nod factor perception induces clathrin-mediated endocytosis accompanied by GmSYP111a re-localization into intracellular vesicles. A non-phosphorylatable mutant (*GmSYP111a*^{S8A}) showed markedly reduced internalization and a corresponding decrease in infection events, resulting in impaired IT formation and a phenotype resembling *GmSymRKβ*-RNAi roots. In contrast, a phosphomimetic variant (*GmSYP111a*^{S8D}) displayed partial vesicular recruitment upon infection. Functional analyses further demonstrated that *GmSYP111a*, but not its paralog *SYP111b*, is indispensable for nodule initiation in soybean, with this role conserved in *Lotus japonicus*. Collectively, our results show that GmSymRKβ-mediated phosphorylation of GmSYP111a functions as a molecular switch that links symbiotic signaling to clathrin-dependent endocytosis. This mechanism coordinates localized membrane remodeling at infection sites, parallels the role of KNOLLE in cytokinesis, and highlights how duplication and neo-functionalization of *GmSYP111a* contributed to the evolution of legume-specific symbiotic pathways.

Introduction

Endosymbiotic interactions, such as the legume–rhizobium symbiosis, demand extensive and highly coordinated remodeling of the host cell membrane system. During rhizobial infection of roots, bacteria are guided inward through ITs – tubular invaginations of the root hair cell wall and plasma membrane[1,2]. These structures, and the nascent symbiotic compartments within nodules, require the host to generate new membrane to accommodate the microbes. In fact, infected nodule cells expand their membrane surface area several-fold (up to twentyfold) as they form the symbiosome membrane that envelopes nitrogen-fixing bacteroids[3]. Polar growth processes like IT extension rely on vesicle trafficking: secretory vesicles deliver membrane and cell wall materials to the growing tip, while endocytic pathways likely recycle and reshape the plasma membrane to allow controlled invagination and bacterial containment[2,4]. Despite the central importance of membrane dynamics in symbiotic infection, how these processes are coordinated with symbiotic signal transduction remains poorly understood.

Plants perceive rhizobial *Nod* factor signals at the root hair surface through receptor-like kinases (RLKs). In legumes, specialized LysM-domain RLKs (e.g., termed *NFR1*/*NFR5* in Lotus and soybean) bind Nod

factors, and the leucine-rich repeat RLK *SymRK* acts as a co-receptor to initiate the common symbiosis signaling pathway[5]. *SymRK* is essential for both rhizobial and mycorrhizal symbioses[6]. Mutations in *SymRK* abolish nodule formation, highlighting its central role in nodulation[7,8]. However, while decades of research have elucidated many downstream genetic requirements of *SymRK*-mediated signaling, the direct mechanistic connections between these symbiotic receptors and the membrane trafficking machinery remain poorly understood. Notably, several plant RLKs undergo ligand-induced endocytosis as part of their signaling regulation (e.g., BRI1, which continues to signal from endosomes after internalization[9]). SymRK is also relocalized into endosomal puncta upon Nod factor stimulation[6], suggesting that receptor internalization may modulate signaling. Nevertheless, it is still unclear whether SymRK—or any plant RLK—actively regulates vesicle trafficking events, as opposed to functioning primarily as cargo of endocytosis.

Membrane fusion during vesicle trafficking is executed by SNARE proteins, which are key determinants of specificity in exocytosis and endocytosis. Many SNAREs fulfill fundamental roles in plant growth; for instance, the Qa-SNARE *KNOLLE* (*AtSYP111*) is a cytokinesis-specific syntaxin required for cell plate formation during Arabidopsis embryogenesis[10,11]. Emerging evidence suggests that certain SNARE components are also deployed in symbiotic infection. In *Medicago truncatula*, two homologous v-SNAREs (*VAMP721d* and *VAMP721e*) are specifically required for IT progression and for the formation of symbiosomes (the membrane-bound organelle-like compartments housing rhizobia)[12]. Silencing these exocytotic SNAREs blocks the release of bacteria into host cells without affecting overall nodule organogenesis[12]. These observations underscore that a dedicated vesicle trafficking pathway underpins bacterial accommodation in legumes. However, it remains unclear how the symbiotic signaling pathway orchestrated by RLKs might interface with this vesicle trafficking machinery.

To address this gap, we employed the Kinase Client (KiC) assay, an in vitro synthetic peptide phosphorylation platform coupled with LC-MS/MS that enables the identification of direct protein substrates for purified kinases[13,14]. This assay quantifies kinase activity by monitoring spectral counts of phosphorylated versus unphosphorylated peptides, offering high sensitivity and specificity with a favorable signal-to-noise ratio. To broaden its utility, an 8k synthetic peptide library was generated, each peptide designed as a 20-mer and enriched for phosphorylation sites conserved across angiosperms, thereby capturing functionally important residues and facilitating kinase substrate discovery across diverse plant species[15].

In this study, we discovered a direct molecular coupling between Nod factor signaling and the host membrane-trafficking apparatus. We identified *GmSYP111a*, a soybean Qa-SNARE, as a legume-specific homolog of *KNOLLE* that is induced during rhizobial infection. GmSYP111a localizes to the plasma membrane of infected root hairs and displays functional divergence from its paralog *GmSYP111b*, which presumably retains the canonical role in cytokinesis. In contrast, *GmSYP111a* appears to have evolved a specialized role in nodulation, as it is specifically induced in root hairs upon rhizobacterial infection, with its upregulation temporally coinciding with IT formation. This raised the hypothesis that *GmSYP111a*

might be directly regulated by symbiotic signaling. Indeed, we found that the cytoplasmic kinase domain of GmSymRKβ physically interacts with GmSYP111a and phosphorylates it at a conserved serine (Ser-8) near the SNARE's N-terminus. This phosphorylation acts as a switch that enables membrane trafficking. In the absence of Nod factor, GmSYP111a resides at the root hair plasma membrane, but upon GmSymRKβ-mediated phosphorylation at Ser-8, GmSYP111a is endocytosed along with the GmSymRKβ receptor complex. In essence, activation of the GmSymRKβ receptor triggers the internalization of itself together with GmSYP111a, thereby physically coupling Nod factor perception to an endocytic remodeling of the plasma membrane.

Our data demonstrate that GmSymRKβ directly phosphorylates GmSYP111a, thereby linking rhizobial signal perception to vesicle dynamics required for IT development. This finding provides a basis for the coordination between signal transduction and membrane trafficking, defining an essential, very early mechanistic step in the rhizobial infection process.

Results

Identification of candidate substrates phosphorylated by GmSymRKβ and functional enrichment analysis

To determine the substrate specificity of the GmSymRKβ receptor kinase, we performed a high-throughput kinase client (KiC) assay using the purified intracellular kinase domain of GmSymRKβ. In this *in vitro* screening, both wild-type and catalytically inactive mutant forms of GmSymRKβ were incubated with ATP and a synthetic peptide library of approximately 8,000 peptides[15], followed by mass spectrometry to detect phosphorylated peptides (Fig. 1a). We assessed overall peptide coverage of the library by mass spectrometry (MS) and confirmed that more than 90% of peptides were reliably detected, demonstrating the robustness of the assay (Fig. 1b). Based on this comprehensive coverage, we then focused on the phosphorylated subset. The resulting peptide spectra were subjected to three sequential filtering steps to ensure high-confidence identifications: Filtration 1, Ascore ≥ 20 and minimum PTM ion intensity ≥ 5%; Filtration 2, Filtration 1 + PSM (peptide-spectrum match) counts ≥ 2; Filtration 3, Filtration 2 + manual spectrum inspection. Through this process, we confirmed that a markedly higher number of peptides were phosphorylated in the wild-type GmSymRKβ condition compared to the kinase-dead mutant plus ATP-only controls, ultimately identifying 69 candidate substrates (Supplementary Table 1).

GO term analysis of the 69 identified proteins revealed significant enrichment of categories related to membrane trafficking and vesicle dynamics, including SNARE complex, exocytosis, endocytosis, and extrinsic component of membrane (Supplementary Table 2 and Figure S1). This indicates that the candidate set is closely associated with membrane remodeling and vesicle transport regulation. Additionally, terms such as kinase inhibitor activity and positive regulation of catalytic activity were significantly enriched, supporting the role of phosphorylation-based regulation of enzymatic activity as a key mechanism. Notably, the candidate set also included remorin, a protein previously characterized as

an interactor of GmSymRKβ in symbiotic signaling[16]. Its recovery as a phosphorylated substrate in the KiC assay provides independent confirmation of the assay's robustness and supports the biological relevance of the identified phosphorylation targets.

Through systematic analysis, one particularly notable target was the soybean Qa-SNARE protein GmSYP111. The phosphorylated peptide identified in a GmSymRKβ-dependent manner was found to align with a homologous N-terminal sequence from the Arabidopsis library, and the phosphorylated Ser-8 residue corresponded to a conserved position in soybean SYP111 (Fig. 1c and Supplementary table 1). These observations support that GmSymRKβ directly phosphorylates this conserved residue of GmSYP111, as demonstrated by *in vitro* kinase assays, consistent with the design of the 8k KiC library enriched for conserved phosphorylation sites across angiosperms [15]. This finding highlighted the need to further investigate the regulatory role of SYP111 in symbiotic signaling and its contribution to IT formation.

GmSYP111a is a Key Regulator of Soybean Nodulation

To dissect the function of *SYP111* in soybean, which encodes two paralogs (*GmSYP111a* and Gm*SYP111b*), we employed *Agrobacterium rhizogenes*–mediated hairy root transformation to generate composite plants and tested individual RNAi constructs alongside an overexpression line (*GmSYP111a*-OX) and an empty vector (EV) control. Following inoculation with *Bradyrhizobium diazoefficiens*, knockdown of *GmSYP111a* caused a significant reduction in nodule number relative to EV (Fig. 2a, b), whereas *SYP111b*-RNAi roots did not differ significantly from controls, despite efficient transcript suppression confirmed by RT–qPCR (Fig. 2c). Overexpression of *GmSYP111a* also did not significantly increase nodule number compared with controls (Fig. 2b).

To test whether SYP111 function is conserved in legumes, we analyzed *Lotus japonicus*, which carries two annotated gene models (*Lj0g3v0109479.1* and *Lj0g3v0109489.1*). RT-PCR showed *Lj0g3v0109479.1* transcripts only in wild-type, while *Lj0g3v0109489.1* was expressed in both wild-type and LORE1 mutants (Figure S2a and b). Full-length cDNA amplification matched the predicted genomic size, confirming *Lj0g3v0109479.1* encodes an intact Qa-SNARE (Figure S2b) and correcting prior annotation errors. A LORE1 insertion mutant (*30098745*) exhibited a clear reduction in nodulation after *Mesorhizobium loti* inoculation compared with Miyakojima MG-20 (Figure S3a, b). Root length was unaffected (Figure S3c), and no cytokinetic defects were observed, unlike the embryo-lethal Arabidopsis *knolle* mutants[11]. This absence of developmental defects likely reflects residual expression of a truncated C-terminal product retaining the SNARE domain (Figure S2c). Overall, *SYP111* is conserved in legumes, and *LjSYP111* is essential for nodulation, paralleling the role of *SymRK* in symbiotic signaling.

To further define the role of *GmSYP111a* during rhizobial infection, we quantified infection events—defined here as the combined occurrence of ITs and infection pockets— at 5 days post-inoculation. *GmSYP111a*-RNAi roots displayed a substantial reduction in infection event numbers compared to EV, a phenotype closely resembling that of *GmSymRKβ*-RNAi roots, while *GmSYP111a*-OX roots showed no

significant increase (Fig. 2d, e). These results suggest that *GmSYP111a* contributes to the initiation and/or growth of ITs. The similarity between *GmSYP111a*-RNAi and *GmSymRKβ*-RNAi phenotypes recalls observations in *Medicago truncatula dmi2* (i.e., *SymRK* homolog) mutants, where root hair curling occurs but bacteria are not entrapped and ITs fail to form[17]. Collectively, the data are consistent with a model in which *GmSYP111a* functions in concert with *GmSymRKβ* at an early stage of infection, facilitating bacterial capture within root hair pockets and promoting IT initiation.

GmSYP111a Expression and Plasma Membrane Localization in Soybean Root Hairs

To elucidate the contribution of *GmSYP111a* to the establishment of symbiosis, we first examined its transcriptional behavior across developmental contexts and tissue types. Mining publicly available soybean transcriptome datasets from the BAR database (https://bar.utoronto.ca/) revealed that both *GmSYP111a* and *GmSYP111b* are abundantly expressed in roots and root hairs. Importantly, however, only *GmSYP111a* transcripts exhibited pronounced induction in root hairs following rhizobial inoculation, underscoring its potential specialization in the earliest phases of infection (Figure S4).

To substantiate these *in silico* observations, we engineered a *GmSYP111a* promoter:CFP transcriptional reporter and introduced it into soybean hairy roots. Confocal microscopy confirmed strong reporter activity in root hairs (Fig. 3a). RT–qPCR assays revealed that both *GmSYP111a* and *GmSYP111b* were upregulated in whole-root samples upon inoculation; nevertheless, only *GmSYP111a* showed significant and consistent induction within purified root hair fractions (Fig. 3b). These findings indicate that while both paralogs are transcriptionally responsive to infection cues at the organ level, *GmSYP111a* is uniquely activated in root hairs, consistent with a role in IT development.

We next examined the spatial distribution of GmSYP111a in relation to GmSymRKβ. Transgenic soybean hairy roots expressing YFP–GmSYP111a and GmSymRKβ-GFP under the CvMV promoter revealed strong localization of both proteins at the cell periphery, consistent with plasma membrane association (Fig. 3c). To verify this localization, plasmolysis assays were performed on epidermal cells subjected to 0.8 M mannitol, which caused the fluorescent signals of both fusion proteins to retract from the cell wall, thereby confirming their identity as plasma membrane residents (Fig. 3d). Upon rhizobial inoculation, the distribution of both proteins shifted markedly: in addition to their peripheral signals, numerous punctate intracellular foci appeared, indicative of endocytic internalization (Fig. 3c). Cross-sectional analyses confirmed that these puncta were positioned inside the plasma membrane, validating their identity as endocytic vesicles engaged in symbiotic membrane remodeling (Figure S5).

Collectively, these results demonstrate that *GmSYP111a* is specifically induced in root hairs by rhizobial signals and encodes a protein that resides at the plasma membrane. This combination of infection-responsive transcriptional activation and dynamic membrane association identifies *GmSYP111a* as a key regulatory component responding to early symbiotic signaling.

GmSymRKβ interacts with and phosphorylates GmSYP111a at Ser-8

To dissect the molecular relationship between GmSYP111a and GmSymRKβ, we combined imaging-based interaction assays, biochemical co-precipitation, and kinase activity measurements. In bimolecular fluorescence complementation (BiFC) assays, EYFPN'–GmSYP111a and GmSymRKβ–EYFPC` were transiently co-expressed in *Nicotiana benthamiana* epidermal cells. Robust peripheral YFP fluorescence was consistently observed, confirming a physical association at the plasma membrane (Fig. 4a). Control combinations lacking one partner yielded no signal, excluding artifactual reconstitution. Importantly, site-directed variants of GmSYP111a revealed that both the non-phosphorylatable GmSYP111a^{S8A} and the phosphomimetic GmSYP111a^{S8D} retained detectable BiFC signals with GmSymRKβ.

In addition to GmSymRKβ, we found that both Nod-factor receptors GmNFR1a and GmNFR5a also formed BiFC signals with GmSYP111a when co-expressed in N. benthamiana (Figure S6 a, b). These interactions were consistently localized to the plasma membrane and were detectable across wild-type, S8A, and S8D variants, indicating that GmSYP111a can associate not only with SymRKβ but also with the canonical Nod-factor receptor pair. This additional receptor–syntaxin connectivity suggests that GmSYP111a may participate more broadly in Nod-factor–elicited membrane signaling complexes prior to the engagement of SymRKβ-mediated phosphorylation cascades.

To substantiate these findings, we performed co-immunoprecipitation (Co-IP) assays in soybean hairy roots. FLAG–GmSymRKβ was reliably co-precipitated with HA–GmSYP111a^{WT}, whereas unrelated HA-tagged controls did not yield signal. Notably, the extent of co-precipitation was unaffected by the presence or absence of rhizobial infection (Fig. 4b). Both GmSYP111a^{S8A} and GmSYP111a^{S8D} were also able to co-precipitate GmSymRKβ (Fig. 4c), mirroring the BiFC observations in heterologous leaf tissue and reinforcing that basal physical interaction is preserved across mutant variants.

Extending the analysis to soybean root hairs at 5 dpi, both WT GmSYP111a and the phosphomimic mutant (GmSYP111a^{S8D}) exhibited BiFC signals at IT membrane sites as well as at the root hair plasma membrane, whereas we failed to detect IT membrane signals in the S8A mutant. (Fig. 4d).

To rigorously determine whether *GmSymRKβ* directly phosphorylates *GmSYP111a*, we performed *in vitro* kinase assays using purified recombinant proteins. The cytoplasmic kinase domain of *GmSymRKβ* (residues 261–616; *GmSymRKβ*-CD) was expressed as a GST fusion, and His-tagged GmSYP111a^{WT} and GmSYP111a^{S8A} were produced as soluble substrates. Upon incubation with [γ-^{32P}] ATP, SDS–PAGE and autoradiography revealed robust phosphorylation of GmSYP111a^{WT} by GmSymRKβ-CD, whereas the catalytically inactive SymRK^{D734N} kinase-dead mutant showed no detectable activity, establishing the specificity of the reaction (Fig. 5a). The authenticity of this phosphorylation was confirmed by λ-phosphatase treatment, which abolished the radiolabel (Fig. 5b). Replacement of Ser-8 with Ala (GmSYP111a^{S8A}) resulted in a pronounced loss of phosphorylation compared with WT (Fig. 5c), and quantitative analysis across independent replicates demonstrated a consistent and significant reduction

in phosphorylation efficiency (Fig. 5d). The residual signal, although reduced compared with WT, was still detectable and likely reflects phosphorylation at additional residues within GmSYP111a. These findings establish Ser-8 as the dominant phosphorylation site of GmSYP111a targeted by GmSymRKβ-CD.

Together, these experiments establish GmSYP111a as a direct and physiologically relevant substrate of GmSymRKβ, with Ser-8 serving as the predominant phosphorylation site. Phosphorylation at this residue does not disrupt the interaction between GmSYP111a and GmSymRKβ, suggesting that its functional impact is mediated through alternative regulatory mechanisms rather than by abolishing binding.

Nod factor signaling and phosphorylation-dependent endocytosis of GmSYP111a and GmSymRKβ

Endocytosis of plasma membrane receptors is a critical regulatory step in legume–rhizobium symbiosis. In *Phaseolus vulgaris*, rhizobia-induced SYMRK endocytosis requires specific phosphorylation sites and an intact YXXØ endocytic motif, thereby modulating both the amplitude and duration of receptor signaling and directly influencing epidermal infection and nodule formation[6]. Building on these findings, we investigated whether the soybean ortholog *GmSymRKβ* undergoes comparable endocytosis and how the SNARE protein GmSYP111a contributes to this process.

To assess the role of Ser-8 phosphorylation in GmSYP111a internalization, we compared the subcellular behavior of YFP–GmSYP111a^{WT}, GmSYP111a^{S8A}, and GmSYP111a^{S8D} in soybean root hairs. Under uninoculated conditions, all variants localized predominantly to the plasma membrane. Following rhizobial inoculation, GmSYP111a^{WT} and GmSYP111a^{S8D} redistributed between the plasma membrane and intracellular vesicles, GmSYP111a^{S8A} remained largely confined to the membrane with minimal internalization (Fig. 6a). Quantitative analysis indicated that Ser-8 phosphorylation is necessary for GmSYP111a endocytosis but not sufficient to enhance it on its own, as the phosphomimic did not exceed WT internalization (Fig. 6b).

We next examined whether GmSYP111a internalization is mechanistically coupled to clathrin-mediated endocytosis of GmSymRKβ. Pharmacological inhibition with TyrA23 and cycloheximide (CHX) treatment following rhizobial inoculation caused a marked reduction in WT GmSYP111a internalization, reaching levels similar to the GmSYP111a^{S8A} mutant (Fig. 6c, d). Consistent with prior work in *Phaseolus vulgaris*, GmSymRKβ endocytosis was also reduced by TyrA23 treatment[6]. Importantly, in *GmSYP111a*-RNAi roots, GmSymRKβ internalization was strongly suppressed, demonstrating that GmSYP111a is indispensable for the clathrin-mediated uptake of GmSymRKβ (Fig. 6c, d). Super-resolution microscopy revealed that GmSYP111a and GmSymRKβ remain in close nanoscale proximity both before and after rhizobial infection, localizing together within plasma membrane nanodomains and internalized vesicular structures (Fig. 6e). Cross-correlation Ripley's $\widehat{L}(r) - r$ analysis demonstrated that the two proteins clustered more closely than expected from a *uniformly distributed random Monte-Carlo simulation*,

maintaining nanometer-scale association throughout the infection process from the plasma membrane to endocytic compartments (Figure S6).

Our results demonstrate that phosphorylation at Ser-8 promotes GmSYP111a internalization and couples this process to the clathrin-mediated endocytosis of GmSymRKβ, with their nano-scale vesicular co-localization supporting the view that they operate as a functional module during the early stages of IT development.

Discussion

Evolutionary Divergence of SYP111 Paralogs in Legumes

Soybean harbors two closely related SYP111 paralogs, GmSYP111a and GmSYP111b, which have diverged in function. *GmSYP111a* is strongly induced during rhizobial colonization and is essential for efficient IT formation and nodulation, whereas GmSYP111b is constitutively expressed and likely retains the ancestral role in cytokinesis. RNAi-mediated depletion of GmSYP111a drastically reduces ITs and nodules without affecting root cell division, while complete loss of both GmSYP111a and GmSYP111b would likely be embryo-lethal due to failed cytokinesis (as observed in Arabidopsis *knolle* mutants[11]. Thus, we could not recover *GmSYP111a/b* double -RNAi hairy roots because depleting the cytokinetic paralog likely prevents the development of transformed roots.

No cytokinesis defects were observed in *GmSYP111a*-deficient soybean roots, presumably due to compensatory functional redundancy. *GmSYP111b* (and possibly *SYP132*) can substitute at the division plane. In Arabidopsis, *SYP132* was shown to partly substitute for *KNOLLE*, and loss of both *KNOLLE* and *SYP132* abolishes cell plate formation[18]. The evolutionary repurposing of *GmSYP111a* for symbiosis appears to involve infection-responsive transcriptional upregulation and novel post-translational control, notably GmSymRKβ-dependent phosphorylation at Ser-8. Conservation analysis in *Lotus japonicus* further supports this interpretation: a LORE1 insertion in *LjSYP111* leads to a pronounced reduction in nodulation but no cytokinetic defects, consistent with residual expression of a truncated C-terminal transcript rather than confirmed protein products. These findings illustrate how legume genomes leveraged gene duplication to co-opt a conserved cytokinetic SNARE for symbiotic innovation, allowing a KNOLLE-type syntaxin to orchestrate IT morphogenesis and nodule development.

IT Formation and Its Parallels with Plant Cytokinesis

The functional role of GmSYP111a in IT morphogenesis highlights a deep mechanistic convergence with plant cytokinesis. GmSYP111a is a close homolog of the Arabidopsis cytokinesis-specific Qa-SNARE KNOLLE, which mediates vesicle fusion at the cell plate through complexes with SNAP33 and VAMP721/722 to drive membrane addition during cytokinesis[10,11,19]. Analogously, our findings suggest that the IT tip represents a specialized polarized membrane domain akin to the cell plate. In both contexts, exocytosis supplies new membrane and cell wall polysaccharides, while clathrin-mediated

endocytosis (CME) retrieves excess membrane and fine-tunes receptor activity. Inhibition of endocytic components disrupts cell plate maturation[20], and in the symbiotic context, perturbation of GmSYP111a phosphorylation compromises IT formation, mirroring these cytokinetic defects.

Biochemical and imaging assays identified GmSYP111a as a substrate phosphorylated by GmSymRKβ at Ser-8. In addition, kinase assays revealed SNAP25-like Qbc-SNAREs (e.g., Glyma.17G076600 and Glyma.05G023100) as putative interactors, suggesting that GmSYP111a may assemble into symbiotic SNARE complexes with Qbc-SNARE partners (Supplementary Table 1). This conceptually mirrors the KNOLLE–SNAP33–VAMP721/722 complexes that drive cell plate formation in Arabidopsis cytokinesis[19], even though direct evidence for corresponding R-SNARE partners in the symbiotic context is lacking. Furthermore, GmSymRKβ undergoes infection-induced endocytosis in a manner dependent on GmSYP111a phosphorylation, suggesting that this phosphorylation-coupled CME attenuates receptor signaling while promoting proper infection thread progression. Direct evidence confirms that NFR1 undergoes infection-induced endocytosis, and stabilization in membrane nanodomains further supports a conserved role for CME in symbiotic signaling[21,22]. Together, these data position GmSYP111a as a central coordinator, integrating Nod factor signaling, exocytic delivery and endocytic recycling to sustain polarized IT formation.

A New Paradigm for Receptor Kinase–SNARE Regulation

Plant receptor kinases (RKs) classically initiate cytosolic kinase cascades (e.g., MAPKs) and transcriptional programs, and direct control of vesicle-trafficking components is considered uncommon. An instructive analogy comes from brassinosteroid signaling, where the BR receptor BRI1 phosphorylates its inhibitor BKI1, driving BKI1's dissociation from the plasma membrane and enabling downstream signaling[23]. Nonetheless, emerging evidence indicates that receptor-proximal kinases can directly modulate SNARE machinery. For example, in Arabidopsis guard cells, the receptor-like cytoplasmic kinase LKS4 phosphorylates the Qa-SNARE SYP121 (PEN1) to promote SNARE-complex assembly[24].

Against this backdrop, our data support a model in which the symbiotic LRR-RLK GmSymRKβ directly phosphorylates the SNARE GmSYP111a at Ser-8. Crucially, receptor internalization in this context proceeds via clathrin-mediated endocytosis (CME)—as demonstrated in legumes by the requirement for an AP2-type YXXΦ endocytic motif in SYMRK and the sensitivity of SYMRK endocytosis to CME inhibitors (tyrphostin A23 and ikarugamycin)[6]. As infection advances, we propose that internalized SymRK–SYP111a complexes are recycled through the trans-Golgi network/early endosome (TGN/EE) system and subsequently redirected to the infection-thread (IT) membrane. This recycling route parallels the behavior of the Nod-factor receptor kinase LYK3, which exhibits infection-dependent vesicular accumulation and later redistribution along ITs in *Medicago truncatula*[21]. Notably, receptor stabilization within SYMREM1/FLOT4 nanodomains preserves signaling competence by preventing premature CME

and degradation[25], whereas the ensuing endocytic–exocytic cycling provides a mechanism to spatially reposition active receptor modules at the growing IT tip[4,12].

Although syntaxins such as SYP111a are classically defined as exocytic Qa-SNAREs, growing evidence indicates that they can also participate in endocytic remodeling. In Arabidopsis, the plasma-membrane SNARE SYP132 regulates the clathrin-mediated endocytosis of the H^+-ATPase AHA1, and altering SYP132 abundance changes the efficiency of AHA1 internalization [26]. This finding highlights the ability of certain syntaxins to function at the boundary between fusion and fission, influencing membrane curvature and retrieval. By analogy, phosphorylated GmSYP111a may tether SymRK-enriched plasma-membrane regions and promote curvature-driven invagination through the same SNARE machinery that normally mediates vesicle fusion. In this capacity, SYP111a likely acts as a hybrid remodeling SNARE that coordinates local exocytic supply with endocytic uptake, generating a self-sustaining cycle of membrane turnover that supports SymRK internalization and compartmentalized signaling.

In this conceptual framework, the SymRK–SYP111a complex likely functions analogously to NFR1/LYK3, undergoing dynamic transitions between nanodomain confinement, CME-mediated internalization, and polarized recycling. Such coupling of receptor phosphorylation, endocytic routing, and vesicle redeployment would integrate Nod-factor perception with localized membrane remodeling, ensuring continuous signaling and sustained IT elongation during symbiotic invasion.

Phospho-SYP111a converts symbiotic receptor clusters into trafficking modules

Our findings suggest that GmSYP111a co-localizes with GmSymRKβ in nanometer-scale clusters at the root hair plasma membrane, which are thought to overlap with nanodomain-based receptor assemblies scaffolded by SYMREM1 and FLOT4. This suggestion is consistent with models positioning Nod factor receptors in nanodomains[25,27,28]. Consistent with this view, an RLK (RinRK1) promotes NFR1/NFR5 accumulation at root hair tips through Flotillin association, linking receptor signaling to nanodomain organization in legumes[29]. This arrangement implies that legumes strategically pre-position symbiotic receptors in specialized membrane regions to ensure rapid and spatially confined responses to rhizobial signals.

A central issue raised by these results is how phosphorylation at Ser-8 of GmSYP111a by GmSymRKβ alters the dynamics of the receptor–SNARE complex. Phosphorylation of plant Qa-SNAREs by kinases can indeed influence their assembly with partners; for example, in Arabidopsis guard cells the RLCK LKS4/SGN1 phosphorylates SYP121, enhancing its pairing with VAMP722[24]. Moreover in legumes, clathrin heavy chain participates in Nod factor signaling and IT formation, supporting a mechanistic link between receptor activation and clathrin-mediated endocytosis[22]. Thus, we propose that GmSymRKβ-dependent phosphorylation does not abolish the GmSymRKβ–GmSYP111a interaction but likely alters complex conformation to expose GmSYP111a to new interactions, reprogramming signaling assemblies into trafficking modules.

Genetic perturbations further underscore this interpretation. The non-phosphorylatable GmSYP111a^{S8A} variant remained at the plasma membrane together with GmSymRKβ, showed little internalization, and dramatically reduced IT formation—phenocopying the *GmSymRKβ*-RNAi lines. Conversely, GmSYP111a^{WT} and GmSYP111a^{S8D} were retained at the plasma membrane under mock conditions. This outcome implies that Ser-8 phosphorylation is necessary but not sufficient for endocytic uptake, and that additional infection-dependent cues—such as lipid remodeling, adaptor engagement, or vesicle scission—are likely required for full internalization (consistent with clathrin-associated endocytic steps observed in *Lotus* root hairs)[22]. Moreover, evidence supports a combinatorial phospho-code on GmSYP111a: in vitro kinase assays retain residual phosphorylation when Ser-8 is substituted, indicating additional sites (Fig. 5c,d), and in vivo phosphoproteomics detects phosphorylation of Ser-128 within the SNARE motif under mock conditions[30], together suggesting that infection-evoked Ser-8 phosphorylation operates atop basal Ser-128 to modulate endocytic competence and partner selection.

Proposed model summary: linking signaling with membrane trafficking

Based on the preceding findings, we propose a model in which the SymRK–SYP111a complex orchestrates the integration of Nod factor signaling with plasma membrane remodeling throughout infection thread (IT) initiation and elongation (Fig. 7a,b,c).

(1) Phosphorylation-driven endocytic switch (Fig. 7a): Upon Nod factor perception, SymRKβ phosphorylates SYP111a at Ser8 within the Habc domain. This phosphorylation disrupts the stable orientation of the receptor complex within the nanodomain and redirects it to clathrin-coated pits, enabling clathrin-mediated endocytosis (CME). Such phosphorylation-dependent reconfiguration of SNARE domains is predicted to alter the electrostatic landscape and structural conformation of the Habc region, thereby modulating binding capacity to endocytic adaptors. Evidence from legumes underscores the biological significance of this mechanism: the CHC1–ROP6–NFR module in Lotus japonicus is indispensable for IT formation[22], while Medicago truncatula LYK3 undergoes infection-dependent redistribution and internalization within REMORIN/FLOTILLIN nanodomains [21,25]. Analogous regulation in Arabidopsis demonstrates that SYP132 governs the endocytosis of the proton pump AHA1 and aquaporin PIP2;1, requiring intact Habc domain function [26].

(2) Infection pocket establishment (Fig. 7b): At the root hair tip, the SymRK–SYP111a complex is proposed to cooperate with REMORIN/FLOTILLIN scaffolds and the CHC1–ROP6–NFR signaling axis to coordinate endocytic and exocytic flows. Following phosphorylation, SYP111a is redirected toward CME foci where selective uptake of receptors and lipid domains likely occurs, while in parallel, exocytosis mediated by VAMP721 and Qbc-SNARE partners deliver membrane and cell wall precursors. The combined activity is hypothesized to generate the infection pocket, a plasma membrane–continuous invagination that accommodates bacterial entry. Genetic and pharmacological studies showing that perturbation of clathrin or actin dynamics disrupts pocket initiation reinforce the functional importance of cytoskeleton-coupled CME at this stage[22,31].

(3) IT elongation and maintenance of symbiotic signaling (Fig. 7c): During IT elongation, the SymRK–SYP111a module appears to sustain a spatially segregated trafficking circuit involving forward-directed secretion and rear-end retrieval. Drawing on parallels with cytokinetic and tip-growing cells, we propose that SYP111a cooperates with VAMP721-type SNAREs and exocyst subunits to drive polarized exocytosis at the IT tip, analogous to the KNOLLE–VAMP721–SNAP33 complex in *Arabidopsis* cytokinesis[19]. Conversely, CME components such as CHC1, AP2/TPLATE, and DRP1/2 likely mediate membrane recycling from the trailing IT region, consistent with the conserved roles of the TPLATE complex and dynamin-related proteins in plant endocytosis [20,32]. Although these associations are drawn by analogy with other plant systems and require direct validation in legumes, they provide a plausible framework for understanding polarized IT growth. Recycled cargo is routed through the TGN/early endosome and returned to the tip, ensuring replenishment of receptors and maintaining signaling capacity. The observed longitudinal distribution of SymRK along the IT membrane (Figure S4d) supports a model in which continuous Nod factor perception and Ca^{2+}–CCaMK–CYCLOPS/IPD3 signaling sustain IT extension[4,33]. Consistent with this view, exocytic and endocytic trafficking have been observed at infection thread release sites, where VAMP721d/e–SYP132 SNAREs and clathrin-associated components coordinate bacterial release and membrane remodeling[12,34], indicating that active membrane turnover and internal Nod factor–dependent signaling are maintained throughout IT progression.

In summary, the phosphorylation of SYP111a at Ser8 by SymRKβ establishes a direct molecular link between Nod factor receptor kinase signaling and the trafficking machinery of the plasma membrane. This coupling provides a mechanistic explanation for how legumes synchronize Nod factor perception with dynamic cycles of endocytosis and exocytosis, thereby enabling the spatial precision and temporal continuity required for infection thread initiation and elongation.

Materials and Methods

Plant Materials, Growth Conditions, and Bacterial Strains

Soybean (*Glycine max* cv. Williams 82) seeds were surface-sterilized and germinated on sterilized germination paper under controlled growth conditions (16 h light/8 h dark, 26°C/23°C light/dark, 80% relative humidity). For nodulation assays, seedlings were inoculated with *Bradyrhizobium diazoefficiens* USDA110 cultured in HM medium[35]. Bacterial cells were harvested at mid-log phase, washed, and resuspended to an OD600 of 0.1 in sterile water before inoculation. For *Lotus japonicus* assays, Miyakojima MG-20 wild-type plants and LORE1 insertion mutant lines were surface-sterilized, germinated on 0.8% agar plates, and transferred to growth pouches under controlled environmental conditions (16 h light/8 h dark, 23°C/20°C Day/night). Seedlings were inoculated with *Mesorhizobium loti* MAFF303099 grown in YEM medium at 28°C to an OD600 of 0.05, washed twice with sterile water, and resuspended for root inoculation. Plants were maintained in nitrogen-free B&D medium, and nodulation phenotypes were assessed at 3 weeks post-inoculation.

Cloning and Plasmid Construction

The cytoplasmic kinase domain of GmSymRKβ (GmSymRKβ-CD) was cloned into pGEX-5X-1 and expressed as a GST fusion protein, and a kinase-dead mutant (D734N) was generated by site-directed mutagenesis as described previously[36]. The N-terminal cytosolic region of *GmSYP111a* (aa 1–280, lacking the transmembrane domain) was cloned into pET28a(+) via EcoRI/XhoI to yield His–GmSYP111a (1–280), and a phospho-deficient mutant (S8A) was similarly generated. These recombinant proteins were used for *in vitro* kinase and KiC assays.

For promoter activity analysis, a 2-kb fragment upstream of the *GmSYP111a* start codon was inserted into psoyGUS[37] (KpnI/PstI) together with ECFP using Gibson Assembly, generating pCAMGFP_ProSYP111a–ECFP.

For overexpression (OX) and RNA interference (RNAi) constructs, the full-length *GmSYP111a* coding sequence and gene-specific fragments for *GmSYP111a* (180 bp, 5' UTR) and *GmSYP111b* (130 bp, 3' UTR) were cloned into pDONR/Zeo and transferred by LR Clonase II recombination into pCAM-RUBY-OX[38] and pCAM-RUBY-CvMV-GWi[38], respectively.

For bimolecular fluorescence complementation (BiFC), a modified Gateway-compatible vector (pGTQL1211-2) harboring an N-terminal 3×HA–YN173 fusion was generated from pGTQL1211YN[39] by Gibson assembly. *GmSYP111a* (WT, S8A, S8D) and *GmSymRKβ* coding sequences were cloned into pDONR/Zeo and recombined into pGTQL1211-2 and pGTQL1221YC[39], producing HA–YN173–GmSYP111a and GmSymRKβ–YC155 BiFC constructs.

For subcellular localization, a modified vector (pGTQL–3×HA–EYFP) was produced from pGTQ1211YN by inserting PCR-amplified 3×HA and EYFP fragments (XhoI/PacI) using Gibson assembly. *GmSYP111a* variants (WT, S8A, S8D) were recombined via LR Clonase II into pGTQ–3×HA–EYFP to yield YFP–GmSYP111a(WT/S8A/S8D). *GmSymRKβ* was fused with mGFP5 in pCAMBIA1302 (NcoI/BstEII) by Gibson assembly to generate pCAM1302–SymRKβ–GFP.

For co-immunoprecipitation (Co-IP) and super-resolution imaging, a dual-tagged construct expressing FLAG–GmSymRKβ and 3×HA–GmSYP111a under the CvMV promoter was assembled. *GmSymRKβ* and *GmSYP111a* were first cloned into pGWB11 and pGWB15, respectively, via LR Clonase II, and the tagged fragments were amplified and sequentially assembled with the CvMV promoter into pSoyGUS (PacI/PstI) using Gibson Assembly, yielding pCAMGFP–GmSymRKβ–FLAG–3×HA–GmSYP111a. This construct was used for both Co-IP and high-resolution imaging assays. Primer sequences used for cloning are listed in Supplementary Table 3.

Soybean Hairy Root Transformation and Phenotypic Assays

Agrobacterium rhizogenes strain K599 carrying the above constructs was used for hairy root transformation[40]. Transgenic roots were identified by GFP fluorescence or Ruby color. Plants were

inoculated with *B. diazoefficiens* USDA110, and nodules were scored 3 weeks post-inoculation. Infection events (infection pockets and ITs) were quantified at 5 dpi. At least 10 plants per replicate were analyzed, and three independent biological replicates were performed.

Gene Expression Analysis

Total RNA was extracted from soybean root tissues using TRIzol reagent (Invitrogen). cDNA was synthesized with M-MLV reverse transcriptase (Promega). Quantitative real-time PCR was performed using SYBR Green PCR master mix (ABI) on a Bio-Rad CFX96 system. Expression levels were normalized to the soybean *Cons6* reference gene[41].

Confocal Microscopy

Roots expressing YFP–GmSYP111a and GFP–GmSymRKβ were imaged using a Leica TCP SP8 confocal microscope. For plasmolysis assays, roots were treated with 0.8 M mannitol for 10 min before imaging. Infection-dependent localization and internalization were monitored at 5 dpi. Images were processed using Fiji software. For inhibition of endocytosis hairy roots expressing fluorescently tagged *GmSYP111a* and *GmSymRKβ* were treated with 100 μM tyrphostin A23 and 50 μM cycloheximide for 1 h prior to inoculation. Endocytic internalization was quantified by confocal microscopy.

Bimolecular Fluorescence Complementation (BiFC)

GmSYP111a and *GmSymRKβ* BiFC constructs were co-infiltrated into *Nicotiana benthamiana* leaves. YFP fluorescence was visualized at 48 hpi with confocal microscopy. Negative controls included empty vectors and split-YFP constructs without one partner.

Co-immunoprecipitation (Co-IP) and Western Blotting

Protein extracts from hairy roots expressing FLAG–GmSymRKβ and HA–GmSYP111a variants were immunoprecipitated with anti-HA affinity gel. Immunoblotting was performed with anti-HA-HRP and anti-FLAG-HRP antibodies. Detection was carried out using ECL chemiluminescence (Invitrogen iBright 750).

Purification of GST- or His-tagged proteins Using Affinity Chromatography

Rosetta™ (DE3) competent cells (Novagen) transformed with the recombinant plasmid were induced with 0.1 mM isopropyl-β-D-1-thiogalactopyranoside (IPTG) for the expression of GST- or His-tagged proteins. Following incubation for 4 h at 22°C, cells were pelleted by centrifugation at 4,000 × g for 10 min. After removing the supernatant, the cell pellet was immediately frozen in liquid nitrogen and thawed on ice. GST-tagged SymRKb proteins (GST-SymRKb-CD) were purified using a lysis buffer containing 50 mM Tris-HCl (pH 8.0), 150 mM NaCl, 0.2 mM PMSF, 1 mM DTT, 1 mM EDTA, 0.25 mg/L lysozyme, 1% Triton X-100, and protease inhibitor (Thermo Scientific, PIA32955). His-tagged Syntaxin proteins were extracted using the same buffer, except that it contained 300 mM NaCl and without EDTA. The resuspended cell lysate was sonicated twice for 4 min each at 4°C with an amplitude of 5 and a duty cycle of 50%, followed by centrifugation at 12,000 × g for 30 min. The resulting supernatant was

collected, and GST- or His-tagged proteins were purified using Glutathione resin (GenScript, #L00206) or TALON metal affinity resin (Takara, #635502) according to the manufacturer's instructions. Remove various chemical contaminants (eg., glutathione) from the eluted protein using a VivaSpin concentrator with a 30 kDa molecular weight cut-off (MWCO) and adjust the final protein concentration to approximately 1 µg/µL.

in vitro Kinase Assay

An *in vitro* kinase assay was conducted with slight modifications from previously described protocols (14, 33). For the assay, 2 µg of purified GST or GST-tagged cytosolic domain of SymRKb containing kinase domain (GST-SymRKb-CD) were incubated with 2 µg of His-tagged Syntaxin protein as a substrate in total reaction volume of 25 µL. The reaction buffer contained 20 mM Tris-HCl (pH 7.4), 10 mM $MgCl_2$, 100 mM NaCl, and 2 mM ATP, supplemented with 10 µCi radioactive [γ-^{32}P] ATP. The mixture was incubated at 30°C for 1 h. Reactions containing [γ-^{32}P] ATP were terminated by adding 5 µL of 5 × SDS sample buffer and heating at 100°C for 5 min using a thermomixer (Eppendorf, Hamburg, Germany). Proteins were resolved by electrophoresis on 12% SDS–PAGE gels. Phosphorylated proteins were visualized by autoradiography using a Typhoon FLA 9000 phosphorimager (GE Healthcare) with an exposure time of 12 h. Gels containing radioactive [γ-^{32}P] ATP samples were subsequently stained with Coomassie Brilliant Blue (CBB) to confirm equal protein loading. GST was used as a negative control, and MBP was used as a universal substrate.

Kinase Client (KiC) Assay

The 8k synthetic peptide library was divided into eight pools of 1000 peptides, resuspended in DMSO (~ 50 mM), and diluted to ~ 5 mM, with LC-MS/MS pre-scans confirming detectability. Kinase assays were performed by incubating purified recombinant GST-tagged GmSymRKβ kinase domain (wild-type or kinase-dead) with peptide pools at a 1:1 enzyme-to-substrate ratio (14.72 µg each) in kinase buffer [20 mM Tris–HCl (pH 7.5), 10 mM $MgCl_2$, 5 mM EGTA, 100 mM NaCl, 1 mM DTT] supplemented with 2 mM ATP, in 40 µL reactions at 30°C for 1.5 h with shaking. Reactions were quenched with 1% formic acid in 99% acetonitrile and stored at − 20°C until analysis. Peptides were separated on an EvoSep UHPLC with a PepSep C18 column (15 cm × 75 µm, 1.9 µm) using a 31-min gradient at 100 nL/min and analyzed on a Bruker TimsTOF Pro 2 in PASEF mode (m/z 100–1700). MS/MS spectra were searched with PEAKS Studio 10.0 against a custom FASTA (8k entries) using a 20-ppm precursor and 0.1 Da fragment tolerance, with phosphorylation (Ser/Thr/Tyr) and methionine oxidation as variable modifications. Peptide-spectrum matches were filtered at 1% FDR, and phosphorylation site localization confidence was determined using Ascore, retaining candidates with Ascore ≥ 20, PTM ion intensity ≥ 5%, ≥ 2 PSM counts, and validated spectra. Mass spectrometry proteomics data have been deposited to the ProteomeXchange Consortium via the PRIDE[42] repository under accession PXD068787.

Super-Resolution Imaging

Soybean root hairs expressing FLAG-tagged GmSymRKβ and Ha-tagged GmSYP111a were used for super-resolution imaging. Root hairs were first treated with 0.2% driselase in 2 mM MES (pH 5.7) at 37°C for 15 min to partially digest the cell wall, followed by plasma membrane permeabilization with 1% Triton X-100 in PBS at room temperature for 20 min. Samples were then incubated in blocking buffer (1% BSA, 0.1% Tween-20, 2 mM sodium azide) before antibody staining. Anti-FLAG (1:50) and anti-Ha (1:200) antibodies were applied overnight at 4°C to detect GmSymRKβ and GmSYP111a, respectively, and samples were washed thoroughly with PBS prior to imaging. For microscopy, root hairs were mounted in imaging buffer (50 mM Tris, 10 mM NaCl, 10% glucose, 56 µg/mL glucose oxidase, 34 µg/mL catalase, 1% 2-mercaptoethanol, 1% mercaptoethylamine) on glass-bottom dishes under a coverslip. Super-resolution images were acquired using an Olympus IX-71 equipped with a 100× oil immersion objective, a 542 nm or 488 nm solid-state laser (5 mW/cm²) with appropriate emission filters, and an Andor iXon Ultra 897 EMCCD camera. Image series (512 × 512 pixels, 160 nm per pixel, 8190 frames at 10 fps) were collected and processed with custom MATLAB scripts to identify and cluster blinking events within 20 nm localization precision. Colocalization of GmSymRKβ and GmSYP111a clusters was further analyzed using *iterative closest point* (*ICP*) alignment, and linear protein expression levels were calculated by normalizing detected protein counts against simulated random distributions[43].

Statistical Analysis

All experiments were repeated with at least three independent biological replicates. Data are expressed as mean ± SEM. Statistical significance was determined using two-tailed Student's *t*-tests or one-way ANOVA with Tukey's HSD test (GraphPad Prism v8). A threshold of $p < 0.05$ was considered significant.

Declarations

Acknowledgement

The research was supported by a grant from the National Science Foundation Plant Genome Program (IOS-2048410).

A portion of this research was performed on a project award (10.46936/ltds.proj.2024.61062/60012421) from the Environmental Molecular Sciences Laboratory, a DOE Office of Science User Facility sponsored by the Biological and Environmental Research program under Contract No. DE-AC05-76RL01830.

References

1. Callaham DA, Torrey JG (1981) The structural basis for infection of root hairs of *Trifolium repens* by *Rhizobium*. Can J Bot 59:1647–1664
2. Gage DJ (2004) Infection and Invasion of Roots by Symbiotic, Nitrogen-Fixing Rhizobia during Nodulation of Temperate Legumes. Microbiol Mol Biol Rev 68:280–300

3. Verma DP, Kazazian V, Zogbi V, Bal AK (1978) Isolation and characterization of the membrane envelope enclosing the bacteroids in soybean root nodules. J Cell Biol 78:919–936
4. Fournier J et al (2008) Mechanism of Infection Thread Elongation in Root Hairs of Medicago truncatula and Dynamic Interplay with Associated Rhizobial Colonization. Plant Physiol 148:1985–1995
5. Roy S et al (2020) Celebrating 20 Years of Genetic Discoveries in Legume Nodulation and Symbiotic Nitrogen Fixation[OPEN]. Plant Cell 32:15–41
6. Dávila-Delgado R, Flores-Canúl K, Juárez-Verdayes MA, Sánchez-López R (2023) Rhizobia induce SYMRK endocytosis in Phaseolus vulgaris root hair cells. Planta 257:83
7. Stracke S et al (2002) A plant receptor-like kinase required for both bacterial and fungal symbiosis. Nature 417:959–962
8. Endre G et al (2002) A receptor kinase gene regulating symbiotic nodule development. Nature 417:962–966
9. Russinova E et al (2004) Heterodimerization and Endocytosis of Arabidopsis Brassinosteroid Receptors BRI1 and AtSERK3 (BAK1). Plant Cell 16:3216–3229
10. Lauber MH et al (1997) The Arabidopsis KNOLLE Protein Is a Cytokinesis-specific Syntaxin. J Cell Biol 139:1485–1493
11. Lukowitz W, Mayer U, Jürgens G (1996) Cytokinesis in the Arabidopsis Embryo Involves the Syntaxin-Related KNOLLE Gene Product. Cell 84:61–71
12. Ivanov S et al (2012) Rhizobium–legume symbiosis shares an exocytotic pathway required for arbuscule formation. *Proceedings of the National Academy of Sciences* 109, 8316–8321
13. Huang Y, Thelen JJ (2012) KiC assay: a quantitative mass spectrometry-based approach for kinase client screening and activity analysis [corrected]. Methods Mol Biol 893:359–370
14. Ahsan N et al (2013) A versatile mass spectrometry-based method to both identify kinase client-relationships and characterize signaling network topology. J Proteome Res 12:937–948
15. Kim D et al (2025) Identifying Receptor Kinase Substrates Using an 8000 Peptide Kinase Client Library Enriched for Conserved Phosphorylation Sites. Mol Cell Proteom 24:100926
16. Lefebvre B et al (2010) A remorin protein interacts with symbiotic receptors and regulates bacterial infection. *Proceedings of the National Academy of Sciences* 107, 2343–2348
17. Esseling JJ, Lhuissier FGP, Emons AMC (2004) A Nonsymbiotic Root Hair Tip Growth Phenotype in NORK-Mutated Legumes: Implications for Nodulation Factor–Induced Signaling and Formation of a Multifaceted Root Hair Pocket for Bacteria. Plant Cell 16:933–944
18. Park M et al (2018) Concerted Action of Evolutionarily Ancient and Novel SNARE Complexes in Flowering-Plant Cytokinesis. Dev Cell 44:500–511e4
19. El Kasmi F et al (2013) SNARE complexes of different composition jointly mediate membrane fusion in *Arabidopsis* cytokinesis. MBoC 24:1593–1601

20. Van Damme D et al (2011) Adaptin-like protein TPLATE and clathrin recruitment during plant somatic cytokinesis occurs via two distinct pathways. *Proceedings of the National Academy of Sciences* 108, 615–620
21. Haney CH et al (2011) Symbiotic Rhizobia Bacteria Trigger a Change in Localization and Dynamics of the Medicago truncatula Receptor Kinase LYK3[W][OA]. Plant Cell 23:2774–2787
22. Wang C et al (2015) Lotus japonicus Clathrin Heavy Chain1 Is Associated with Rho-Like GTPase ROP6 and Involved in Nodule Formation. Plant Physiol 167:1497–1510
23. Wang D et al (2017) BKI1 Regulates Plant Architecture through Coordinated Inhibition of the Brassinosteroid and ERECTA Signaling Pathways in *Arabidopsis*. Mol Plant 10:297–308
24. Ding X et al (2024) LKS4-mediated SYP121 phosphorylation participates in light-induced stomatal opening in *Arabidopsis*. Curr Biol 34:3102–3115e6
25. Liang P et al (2018) Symbiotic root infections in Medicago truncatula require remorin-mediated receptor stabilization in membrane nanodomains. Proc Natl Acad Sci U S A 115:5289–5294
26. Xia L, Mar Marquès-Bueno M, Bruce CG, Karnik R (2019) Unusual Roles of Secretory SNARE SYP132 in Plasma Membrane H+-ATPase Traffic and Vegetative Plant Growth1[OPEN]. Plant Physiol 180:837–858
27. Su C et al (2023) Stabilization of membrane topologies by proteinaceous remorin scaffolds. Nat Commun 14:323
28. Haney CH, Long SR (2010) Plant flotillins are required for infection by nitrogen-fixing bacteria. *Proceedings of the National Academy of Sciences* 107, 478–483
29. Zhou N et al (2024) RinRK1 enhances NF receptors accumulation in nanodomain-like structures at root-hair tip. Nat Commun 15:3568
30. Nguyen THN et al (2012) Quantitative phosphoproteomic analysis of soybean root hairs inoculated with Bradyrhizobium japonicum. Mol Cell Proteom 11:1140–1155
31. Qiu L et al (2015) SCARN a Novel Class of SCAR Protein That Is Required for Root-Hair Infection during Legume Nodulation. PLoS Genet 11:e1005623
32. Gadeyne A et al (2014) The TPLATE Adaptor Complex Drives Clathrin-Mediated Endocytosis in Plants. Cell 156:691–704
33. Yano K et al (2008) CYCLOPS, a mediator of symbiotic intracellular accommodation. *Proceedings of the National Academy of Sciences* 105, 20540–20545
34. Limpens E et al (2005) Formation of organelle-like N2-fixing symbiosomes in legume root nodules is controlled by DMI2. *Proceedings of the National Academy of Sciences* 102, 10375–10380
35. Cole MA, Elkan GH (1973) Transmissible Resistance to Penicillin G, Neomycin, and Chloramphenicol in Rhizobium japonicum1. Antimicrob Agents Chemother 4:248–253
36. Tóth K et al (2025) Soybean RIN4 represents a mechanistic link between plant immune and symbiotic signaling. *eLife* 12

37. Hossain MS et al (2019) Characterization of the Spatial and Temporal Expression of Two Soybean miRNAs Identifies SCL6 as a Novel Regulator of Soybean Nodulation. Front Plant Sci 10
38. Song Jhyo et al (2025) Phloem-Specific Translational Regulation of Soybean Nodulation: Insights from a Phloem-Targeted TRAP-Seq Approach. 04.09.647652 Preprint at https://doi.org/10.1101/2025.04.09.647652 (2025)
39. Lu Q et al (2010) Arabidopsis homolog of the yeast TREX-2 mRNA export complex: components and anchoring nucleoporin. Plant J 61:259–270
40. Song J, Tóth K, Montes-Luz B, Stacey G (2021) Soybean Hairy Root Transformation: A Rapid and Highly Efficient Method. Curr Protoc 1:e195
41. Libault M et al (2008) Identification of Four Soybean Reference Genes for Gene Expression Normalization. Plant Genome 1
42. Perez-Riverol Y et al (2025) The PRIDE database at 20 years: 2025 update. Nucleic Acids Res 53:D543–D553
43. Kiskowski MA, Hancock JF, Kenworthy AK (2009) On the Use of Ripley's K-Function and Its Derivatives to Analyze Domain Size. Biophys J 97:1095–1103

Figures

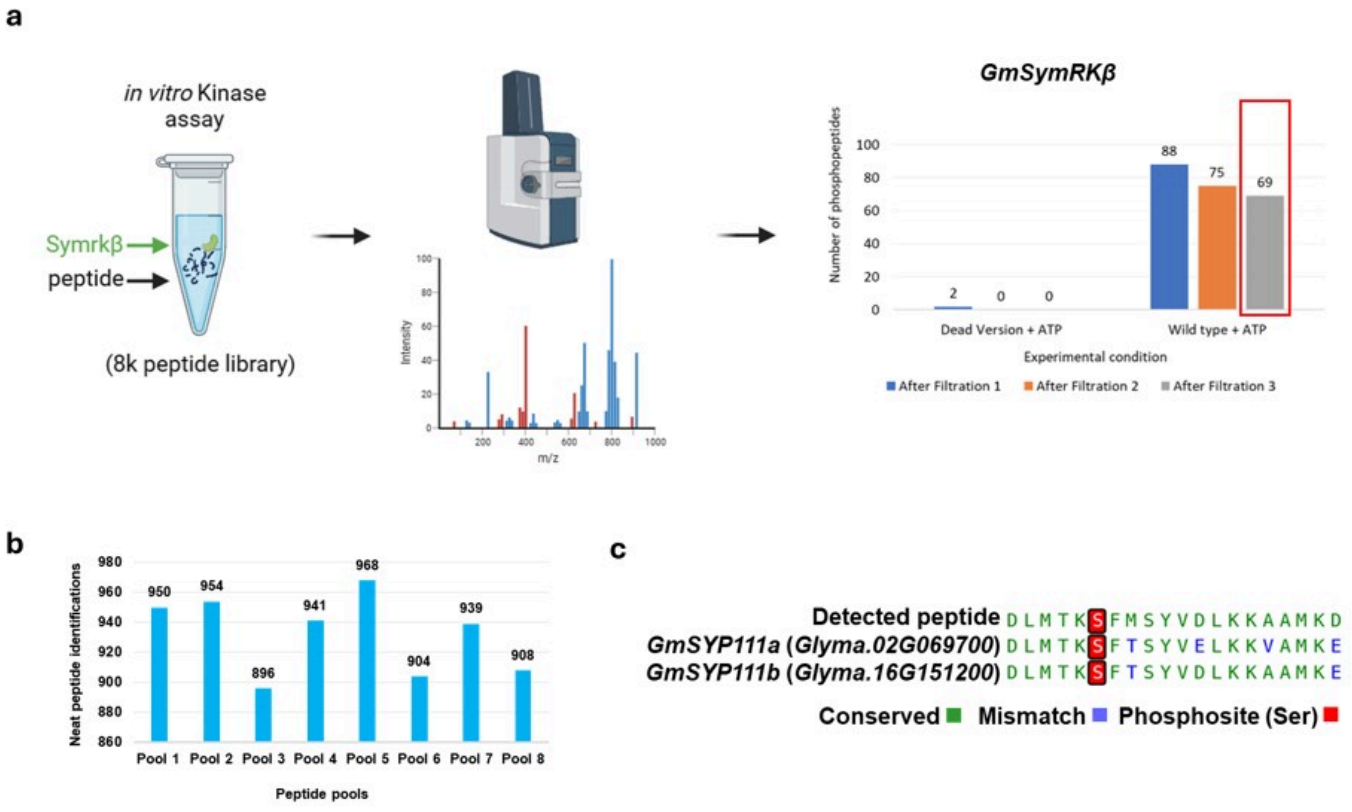

Figure 1

Analysis of phosphorylation by GmSymRK using a kinase client (KiC) assay.

(a) (Left) Schematic diagram of an *in vitro* kinase assay. GmSymRKβ protein (green) was incubated with a synthetic peptide library (8,000 peptides) and ATP. (Middle) The reaction mixture was analyzed by mass spectrometry, and the resulting spectra display peaks corresponding to phosphopeptides with varying m/z values. (Right) Bar graph showing the number of phosphopeptides detected under three experimental conditions: kinase-dead GmSymRKβ + ATP, wild-type GmSymRKβ + ATP, and ATP only. Data are presented after three sequential filtration steps, with the highest number of phosphopeptides observed in the wild-type SymRKβ condition. (b) Distribution of unique phosphopeptide identifications across each 1000-peptide pool from the wild-type + ATP dataset, confirming broad substrate coverage within the peptide library. (c) Identification of GmSYP111a as a candidate substrate of SymRKβ. The phosphorylation site mapped to Ser-8 in the N-terminal region of GmSYP111a, aligned with conserved sequences across homologs.

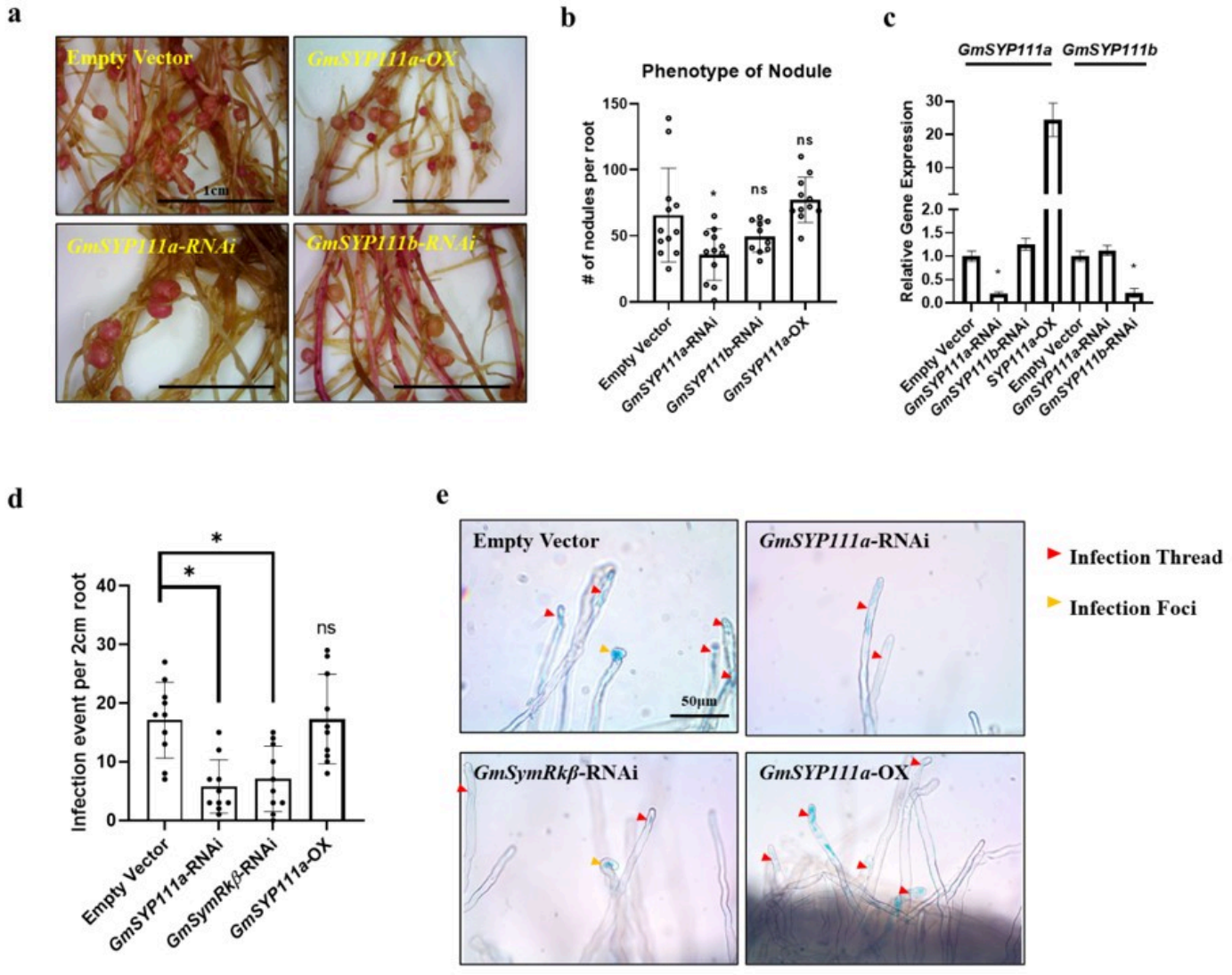

Figure 2

GmSYP111a regulates nodule formation and infection thread development in soybean roots.

(a) Representative images of transgenic soybean hairy roots expressing *GmSYP111a*-OX, *GmSYP111a*-RNAi, *GmSYP111b*-RNAi, or Empty Vector constructs at 21 days post inoculation (dpi) with *Bradyrhizobium diazoefficiens*. (b) Quantification of nodule number per root across the different transgenic lines (n = 8–10). Each dot represents a single biological replicate. (c) Expression levels of *SYP111a* and *SYP111b* in nodules at 21 dpi determined by quantitative RT–PCR. Gene expression was normalized to *cons6*. Bars represent mean ± SD. Statistical significance was determined using unpaired two-tailed Student's *t*-test; $P < 0.05$ was considered significant. (d) Quantification of infection thread (IT) numbers in transgenic roots transformed with empty vector (EV), *GmSYP111a*-RNAi, *GmSymRKβ*-RNAi, and *GmSYP111a*-OX constructs. Data represent mean ± SD from ten biological replicates. Statistical significance was determined using a two-tailed Student's *t*-test. (e) Representative images of GUS-stained root hairs at 5 days post-inoculation with *Bradyrhizobium diazoefficiens* USDA110 carrying the *gusA* reporter. Red arrowheads indicate infection threads; yellow arrowheads indicate infection pockets. Scale bars, 50 μm.

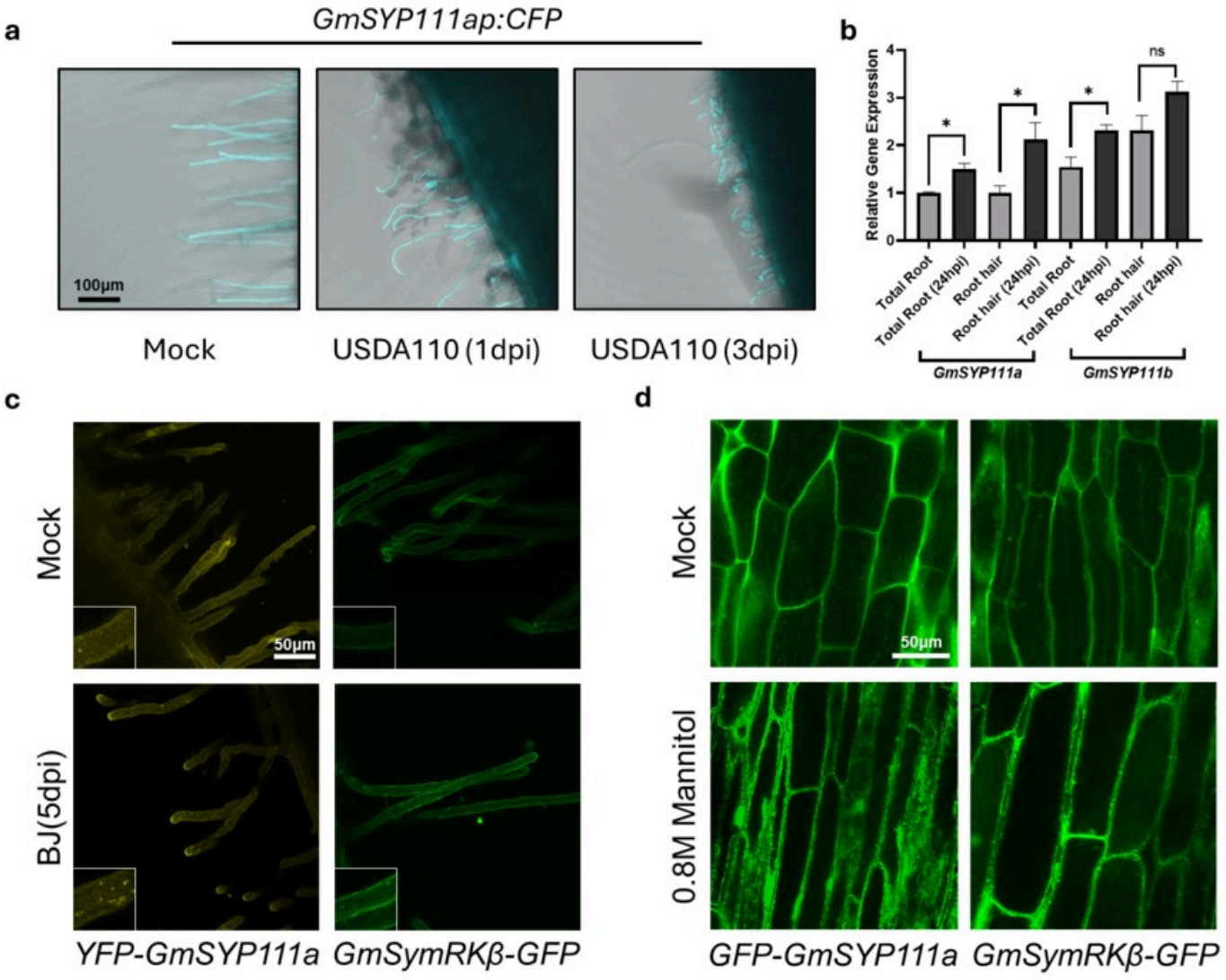

Figure 3

Gene expression and subcellular localization analyses in soybean roots.
(a) SYP111a promoter activity visualized by CFP fluorescence in Agrobacterium rhizogenes–transformed hairy roots, with signal predominantly in root hairs. Scale bar, 100 μm.
(b) RT–qPCR analysis of *SYP111a* and *SYP111b* transcript induction in roots and root hairs following inoculation with Bradyrhizobium diazoefficiens. Right panel: quantification (mean ± s.e.m.; two-sided unpaired Student's t-test). (c) Confocal images showing subcellular localization of SYP111a and SYMRKβ fusion proteins in root hairs. Scale bar, 50 μm. (d) Plasmolysis assay confirming plasma membrane localization of SYP111a and SYMRKβ. Scale bar, 50 μm.

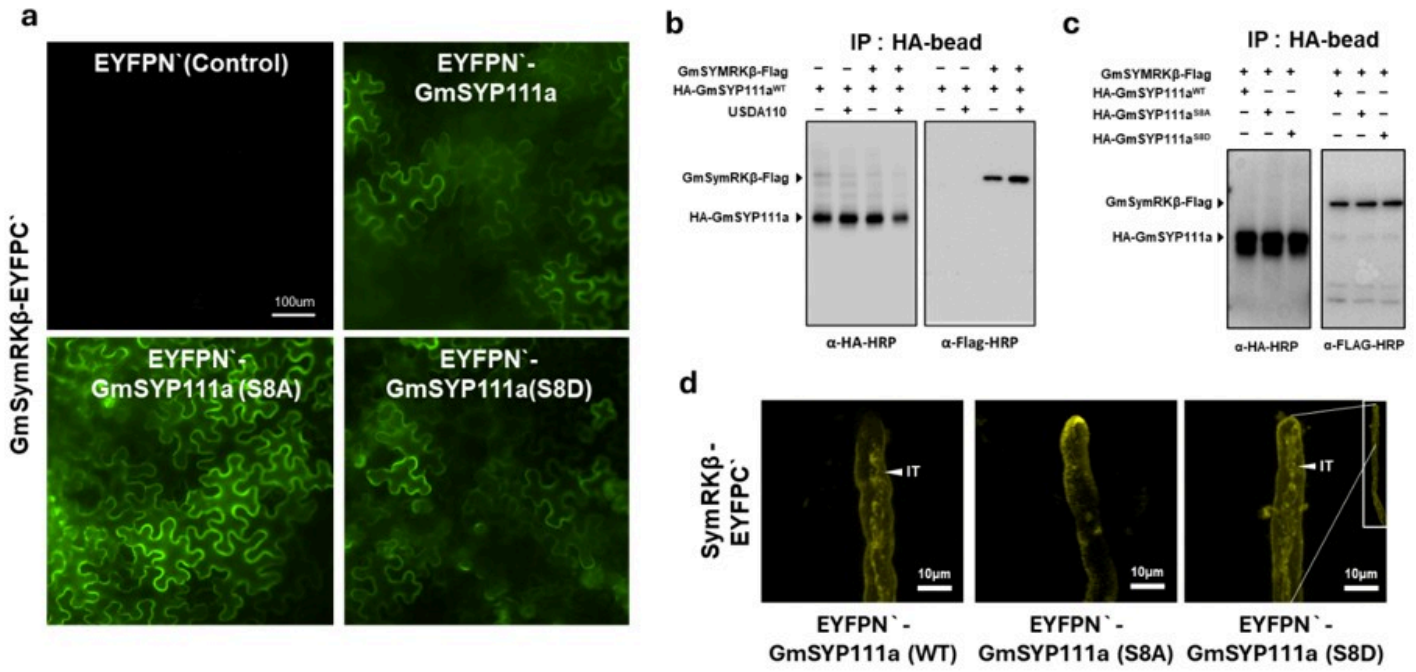

Figure 4

Interaction between GmSYP111a and GmSymRKβ detected by BiFC and Co-IP.
(a) BiFC in *Nicotiana benthamiana* epidermal cells expressing EYFPN'–GmSYP111a wild type, S8A, or S8D together with GmSymRKβ–EYFPC'; EYFPN' alone as control. Scale bars: 100 μm. (b) Co-IP in soybean roots expressing FLAG–GmSymRKβ and HA–GmSYP111a wild type, using samples with or without rhizobacterial inoculation; protein extracts were immunoprecipitated with anti-HA and immunoblotted with anti-FLAG and anti-HA. (c) Co-IP in soybean roots expressing FLAG–GmSymRKβ and HA–GmSYP111a wild type, S8A, or S8D; immunoprecipitation with anti-HA and immunoblot detection with anti-FLAG and anti-HA. (d) BiFC in soybean root hairs at 5 days post-inoculation with rhizobia, expressing EYFPN–GmSYP111a wild type together with GmSymRKβ–EYFPC; infection threads (IT) indicated. Scale bars: 10 μm.

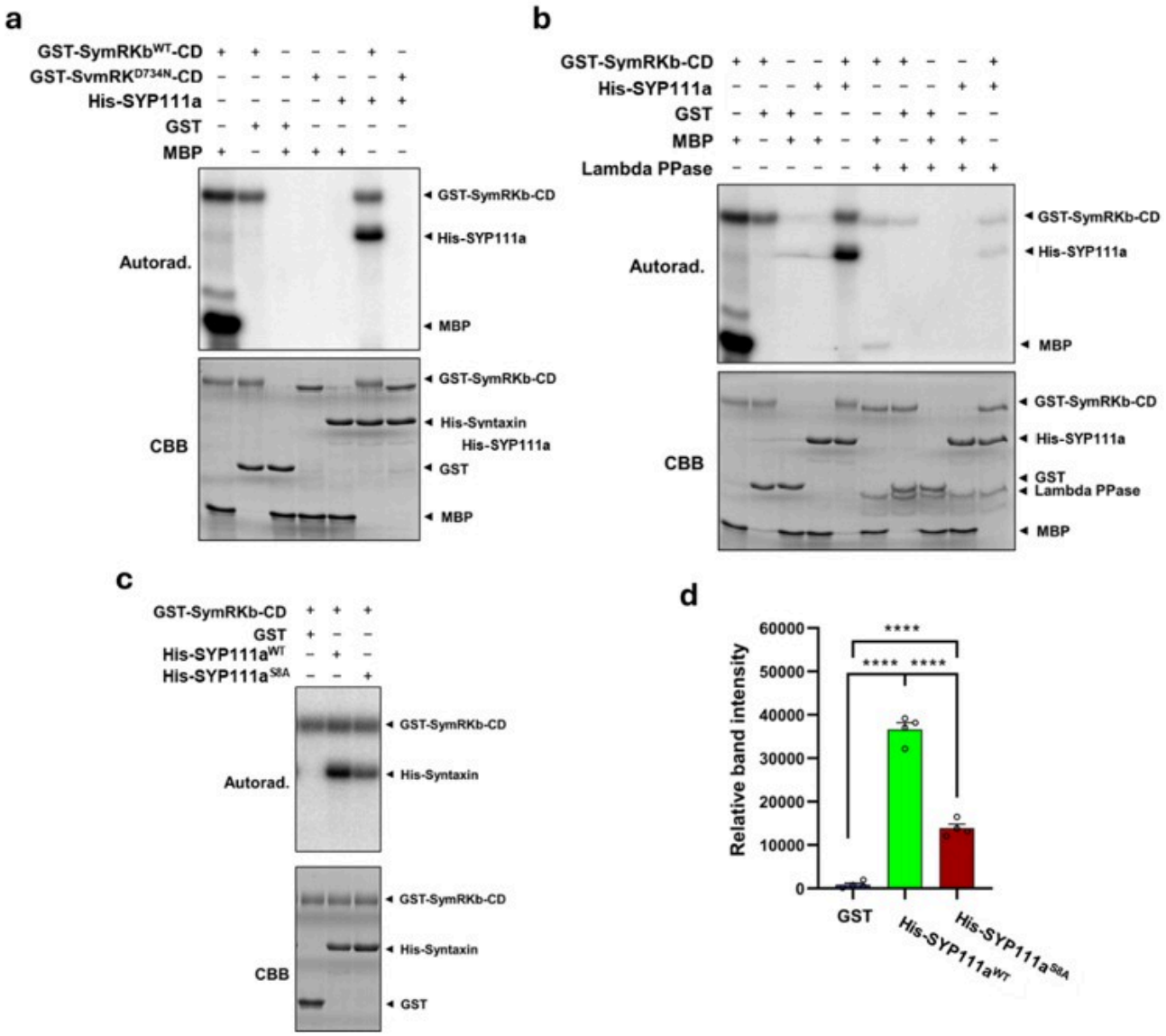

Figure 5

in vitro phosphorylation of GmSYP111a by GmSymRKβ.

(a–b) *in vitro* kinase assay using GST–GmSymRKβ-CD^{WT} or kinase-dead mutant (GST–GmSymRKβ-CD^{D734N}) and His–*GmSYP111a*^{S8A} phospho-deficient mutant or His–GmSYP111a. Purified proteins were incubated with [γ-^{32P}]ATP, separated by SDS–PAGE, and visualized by autoradiography (top panels). Coomassie Brilliant Blue-stained gels are shown as loading controls (bottom panels). (c) Representative autoradiograph showing reduced phosphorylation of His–GmSYP111a^{S8A} by GST–GmSymRKβ-CD. (d) Quantification of phosphorylation intensity normalized to protein loading. Data are presented as mean ± SEM, n = 4 (biological replicates). Statistical significance was determined by one-way ANOVA followed by Tukey's multiple comparisons.

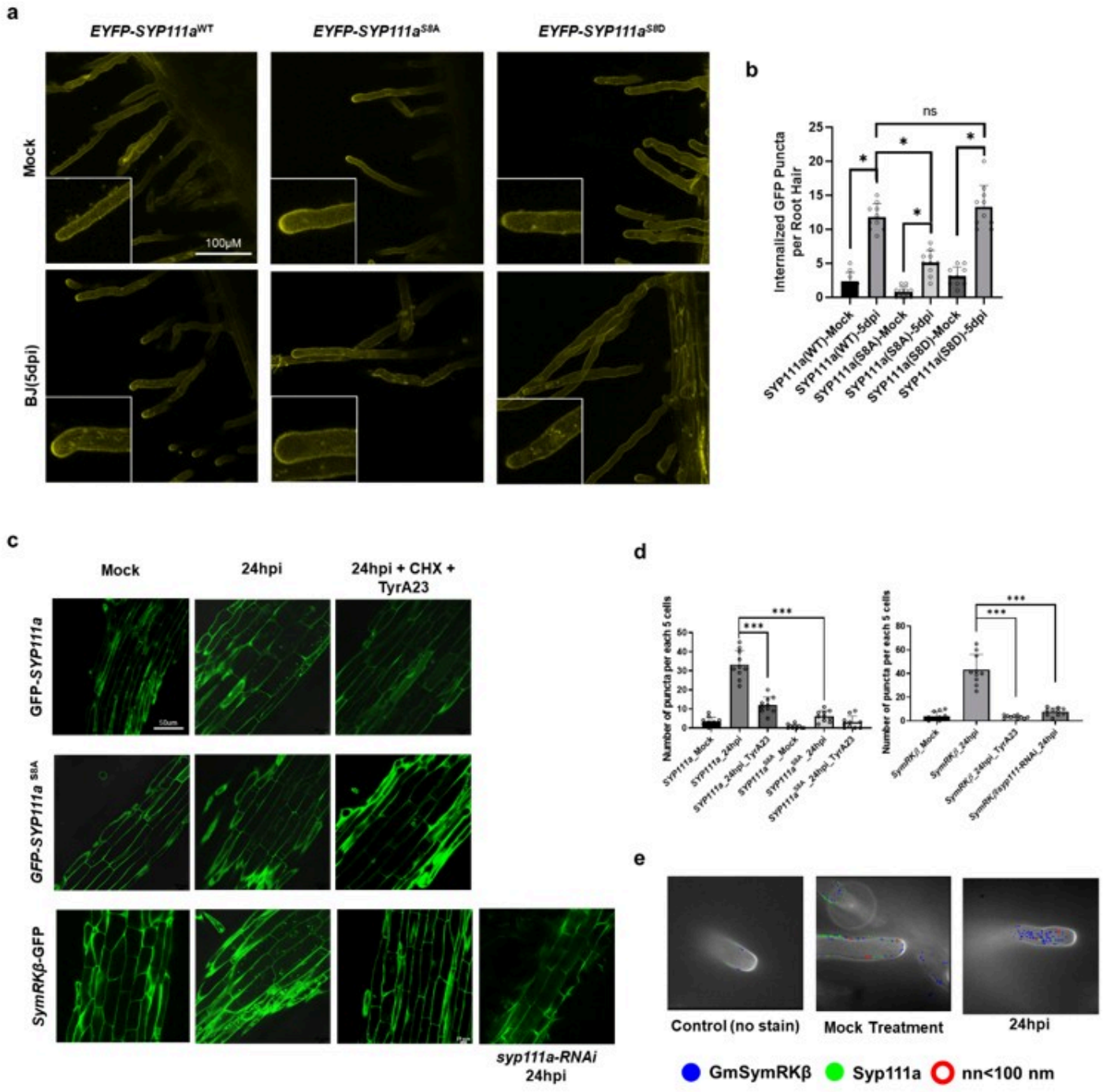

Figure 6

Regulation of GmSYP111a and GmSymRKβ membrane localization and endocytosis during rhizobial infection

(a) Confocal laser scanning microscopy images showing YFP fluorescence of *SYP111a*wild type (WT), phospho-deficient (*S8A*), and phospho-mimic (*S8D*) variants in epidermal cells of soybean roots at 5 days post-inoculation (dpi) with rhizobia or under mock treatment. Insets display magnified views of the root hair tip regions. Scale bar: 100 μm. (b) Quantification of internalized GFP puncta per root hair in *SYP111a* WT, *S8A*, and *S8D* variants under mock or 5 dpi conditions. Data represent mean ± SD from 10

independent biological replicates. Statistical significance was determined using unpaired two-tailed *t*-tests ($P < 0.05$; ns, not significant). (c) Confocal laser scanning microscopy images showing endocytosis of GFP–*GmSYP111a*and *GmSymRKβ*–GFP in epidermal cells of *Glycine max* (Wm82) hairy roots overexpressing the respective constructs, at 24 h post-inoculation with rhizobia. Roots were treated with 100 μM Tyrphostin A23 (TyrA23) and 50 μM cycloheximide immediately after bacterial infection. GFP fluorescence marks plasma membrane localization and internalized endocytic vesicles. Scale bars: 50 μm. (d) Quantification of endocytic vesicles based on the number of GFP-labeled puncta counted from five adjacent epidermal cells per root (n = 10 biological replicates). (e) Super-resolution microscopy images showing subcellular localization of *GmSymRKβ* and *GmSYP111a* in root hair cells. *GmSymRKβ* was detected using anti-FLAG antibody, and *GmSYP111a* was detected using anti-Ha antibody. Scale bars: 10μm. Data in (b) are presented as mean ± s.e.m., with individual data points shown. Statistical significance was determined using two-tailed Student's *t*-test; **P** < 0.01.

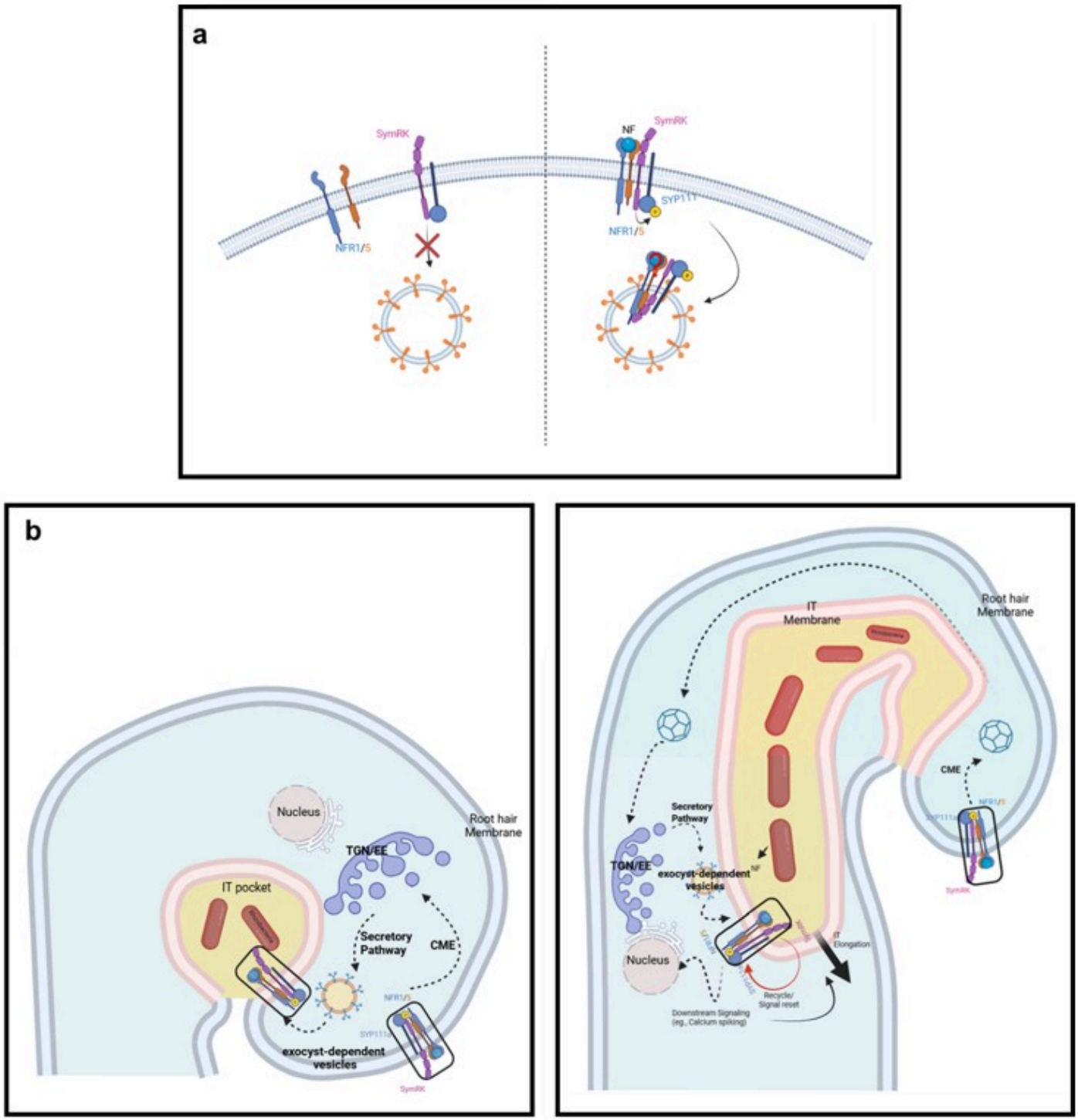

Figure 7

Proposed model for SymRK–SYP111a–mediated coordination of signaling and membrane trafficking during infection thread development.

(a) Phosphorylation-driven CME switch. In the absence of Nod factor (NF), NFR1/5 and SymRK remain at the plasma membrane, but clathrin-mediated endocytosis is inactive because SYP111a is unphosphorylated. Upon NF perception, SymRK phosphorylates SYP111a at Ser-8, enabling the assembly of an NFR1/5–SymRK–SYP111a complex that is recruited into clathrin-coated pits and

internalized. (b) Infection pocket formation. At the root hair tip, the SymRK–SYP111a complex is proposed to coordinate clathrin-mediated endocytosis (CME) with exocyst-dependent exocytosis. Internalization of receptor complexes via CME is coupled with polarized exocytosis of membrane and cell wall precursors through VAMP721/Qbc-SNARE partners. This integrated trafficking activity supports the invagination of the plasma membrane to form the infection pocket that accommodates rhizobacterial entry. (c) IT elongation and signal maintenance. During infection thread elongation, the SymRK–SYP111a module sustains a spatially segregated trafficking circuit. Polarized secretion at the growing tip delivers new membrane and cell wall materials, while CME retrieves receptors and cargo at the trailing IT membrane. Recycled components are routed via the TGN/early endosome (TGN/EE) and redirected to the tip, ensuring receptor replenishment and resetting of Nod factor perception. This recycling sustains downstream signaling, including Ca^{2+} spiking, and enables continuous IT growth.

Supplementary Files

This is a list of supplementary files associated with this preprint. Click to download.

- tableS1.csv
- tableS2.csv
- tableS3.csv
- SupplementaryFigures.docx